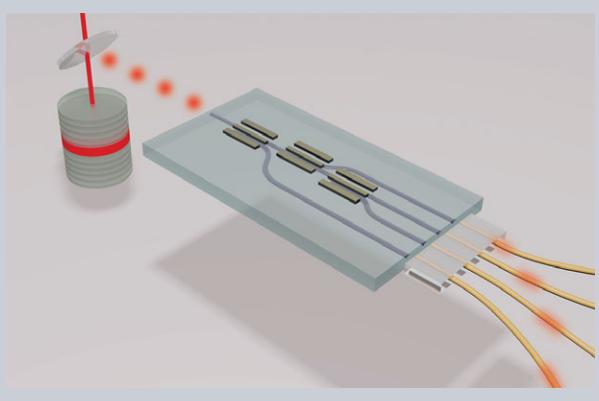**Abstract** A scheme for active temporal-to-spatial demultiplexing of single photons generated by a solid-state source is introduced. The scheme scales quasi-polynomially with photon number, providing a viable technological path for routing n photons in the one temporal stream from a single emitter to n different spatial modes. Active demultiplexing is demonstrated using a state-of-the-art photon source—a quantum-dot deterministically coupled to a micropillar cavity—and a custom-built demultiplexer—a network of electro-optically reconfigurable waveguides monolithically integrated in a lithium niobate chip. The measured demultiplexer performance can enable a six-photon rate three orders of magnitude higher than the equivalent heralded SPDC source, providing a platform for intermediate quantum computation protocols.

Active demultiplexing of single photons from a solid-state source

Francesco Lenzini[1], Ben Haylock[1], Juan C. Loredo[2,3], Raphael A. Abrahão[2], Nor A. Zakaria[2],
Sachin Kasture[1], Isabelle Sagnes[3], Aristide Lemaitre[3], Hoang-Phuong Phan[4],
Dzung Viet Dao[4,5], Pascale Senellart[3,6], Marcelo P. Almeida[2], Andrew G. White[2],
and Mirko Lobino[1,4,*]

A key requirement for large-scale quantum photonic technologies is the availability of reliable sources of multiple indistinguishable single-photons. To date, spontaneous parametric down-conversion (SPDC) sources have been the most widely-used technology in the generation of indistinguishable single-photons. However, the presence of unwanted multiple-photon terms in the SPDC state limits the brightness of high-purity single-photon sources to values lower than 1% [1]. To circumvent this limitation different approaches have been introduced, including active spatial [2, 3], temporal [4, 5], and spatio-temporal [6, 7] multiplexing schemes that combine the outputs of many SPDC sources to create one bright source without deteriorating single-photon purity or indistinguishability [5]–although typically at the cost of a large resource overhead in terms of active optical circuits and single photon detectors since a n-photon heralded SPDC multiplexed source requires n nonlinear crystals and n single-photon detectors.

In comparison, single emitters have the advantage of producing nearly-pure single-photon Fock states. Very recent advances in quantum dot (QD) technologies have resulted in single-photon sources with simultaneously near-perfect purity, near-unity indistinguishability, and high ef-

ficiencies [8, 9]—over an order of magnitude brighter than SPDC sources with equivalent levels of purity and indistinguishability. Thus, quantum dots have now become an attractive platform to develop multi-fold single-photon (multi-photon) sources.

Achieving high indistinguishability and brightness with multiple independent QDs is still a challenge. However, it has been shown that a single QD coupled to a micropillar cavity can emit photons with excellent indistinguishability over long emission timescales [10, 11], meaning that temporal-to-spatial demultiplexing can be used to obtain multi-photon sources. In this work, we implement two important advances towards the realisation of a scalable multifold single-photon source. We first demonstrate the active temporal-to-spatial demultiplexing of a stream of photons to create multi-photon sources with small resource overhead. Secondly, we introduce an integrated zero-buffer active spatial and temporal photonic demultiplexing device, suitable for use with high brightness solid-state sources operating at 932 nm.

Figure 1 schematically depicts our proposed demultiplexing protocol. A temporal stream of single-photons emitted from a quantum dot-micropillar system is actively

[1] Centre for Quantum Dynamics, Griffith University, Brisbane, Australia
[2] Centre for Engineered Quantum Systems, Centre for Quantum Computer and Communication Technology, School of Mathematics and Physics, University of Queensland, Brisbane, Queensland, 4072 Australia
[3] CNRS-C2N Centre de Nanosciences et de Nanotechnologies, Université Paris-Saclay, 91460 Marcoussis, France
[4] Queensland Micro and Nanotechnology Centre, Griffith University, Brisbane, Australia
[5] School of Engineering, Griffith University, Queensland, Australia
[6] Departement de Physique, Ecole Polytechnique, Universite Paris-Saclay, F-91128 Palaiseau, France
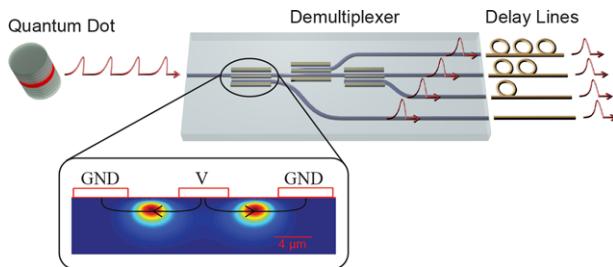*Corresponding Author: e-mail: m.lobino@griffith.edu.au

Figure 1 Scheme for an ideal active spatial-temporal demultiplexing. A stream of single-photons emitted at successive time intervals from a quantum dot coupled to a micropillar cavity are actively routed into different spatial channels by an optical demultiplexer. A set of delay lines at the output can be used to match the arrival times of the single photons. The optical demultiplexer consists of a network of reconfigurable directional couplers with electro-optically tunable splitting ratio. The inset shows the configuration of the electrodes in each directional coupler. The colormap (a.u.) represents the waveguides intensity mode profiles at 932 nm and the black arrows show the direction of the applied electric field.

routed into different spatial channels by an optical demultiplexer. The demultiplexer is an integrated waveguide device with one input and four output channels made of a network of electro-optically reconfigurable directional couplers fabricated on an X-cut lithium niobate substrate by the annealed proton exchange technique [12]. Electrodes are patterned on top of the waveguides as shown in the inset of Fig. 1, and can be used to tune the splitting ratio in the full $0 - 100\%$ range by changing the phase mismatch $\Delta\beta$ between interacting modes [13]. Monolithic integration of the directional coupler network on a single chip is necessary for reduced insertion losses, and with our technology it allows up to 10 output channels in a 5 cm long device.

The n-photon count rate $c_{\mathrm{DM}}(n)$ measured at the output of an n-channel demultiplexer can be expressed as

$$c_{\mathrm{DM}}(n) = R\left[\eta_{\mathrm{SD}}\eta_{\mathrm{det}}\right]^n S_{\mathrm{DM}}(n), \qquad (1)$$

where $\eta_{\mathrm{SD}} = \eta_{\mathrm{QD}}T$ is the product of the source brightness η_{QD}, defined as the probability of emitting one photon at the input of the demultiplexer for each excitation pulse, times the total transmission of the device T. R is the pump rate of the source and η_{det} is the detectors efficiency. $S_{\mathrm{DM}}(n)$ is a parameter which accounts for how the efficiency of the demultiplexing scheme scales with increasing number of photons and it represents the limit of what can be achieved by the demultiplexer with a lossless and deterministic source. Note that the term $[\eta_{\mathrm{SD}}\eta_{\mathrm{det}}]^n$ is intrinsically probabilistic, and will unavoidably result in an exponential decay with photon number. In a probabilistic scheme [14] –made of a network of passive beam splitters– the demultiplexing parameter scales as $S_{\mathrm{DM}}(n)=(1/n)^n$, super-exponentially decreasing with n—a non-scalable approach. In contrast, in an active demultiplexing scheme the scaling is

$$S_{\mathrm{DM}}(n) = \frac{1}{n}\left[\eta_{\mathrm{DM}}^n + (n-1)\left(\frac{1-\eta_{\mathrm{DM}}}{n-1}\right)^n\right], \quad (2)$$

where η_{DM} is the "switching efficiency", defined as the average probability of routing a single photon in the desired channel in each time bin. In the limit of *deterministic* demultiplexing, i.e. $\eta_{\mathrm{DM}} \to 1$, the scaling becomes polynomial in n—thus constituting a *scalable* approach.

The waveguides were fabricated with a 6 μm channel width and a proton exchange depth of 0.47 μm followed by annealing in air at 328 °C for 15 h. These parameters are chosen in order to ensure good overlap with single-mode fiber and single-mode operation at $\sim$930 nm, the emission wavelength of our InGaAs QD. Each directional coupler has a distance between waveguide centres of 8.8 μm and a 4.5 mm length (equal to three coupling lengths), resulting in complete transmission of light into the coupled waveguide when no voltage to the corresponding switching electrodes is applied. Difference from this ideal behaviour is from non-uniform waveguide channel widths, caused by the resolution of the photolithography.

The performance of the demultiplexer is tested in conjunction with a single-photon source based on a QD deterministically coupled to a micropillar cavity [10, 15]. The experimental setup is schematically shown in Fig. 2a: the QD is quasi-resonantly pumped via p-shell excitation with a 905 nm, 80 MHz, 5 ps pulsed Ti:Sapphire laser. The single-photons have a 932 nm emission wavelength and are separated from the pump beam via a dichroic mirror and a 0.85 nm FWHM bandpass filter. Quarter- and half-wave plates are used at the input for polarisation alignment as the waveguides within the demultiplexer guide one (horizontal) polarisation. In our case, this reduces the available photon flux at the input of the demultiplexer by $\sim$50% since the source is only weakly polarised [15], an issue absent if operated with sources engineered to exhibit a large degree of polarization. Photons are injected at the input of the device with a lens of NA = 0.55 and all four outputs are collected with a fibre V-Groove array. Photon-coincidences between the output channels are measured using avalanche photodiodes with 30% average quantum efficiency, and a time-tagging module (TTM). The electrodes of the demultiplexer are driven with a custom-made pulse generator based on a field programmable gate array (FPGA) [16]. The FPGA produces a preset sequence of pulses with varying amplitude voltages that are used to tune the splitting ratio of the directional couplers between on and off values. The driving pulses are synchronized with the clock signal of the Ti:Sapphire laser using internal phase-locked loops (PLL) of the FPGA which provide an adjustable time delay with a low time jitter (300 ps) [16]. The demultiplexer can be actively driven into any configuration by changing the programming of the pulse generator, however as the clocking is derived from the pump laser and not the single photon emission it is not an event-ready reconfiguration. Driving voltages were optimized by maximizing the
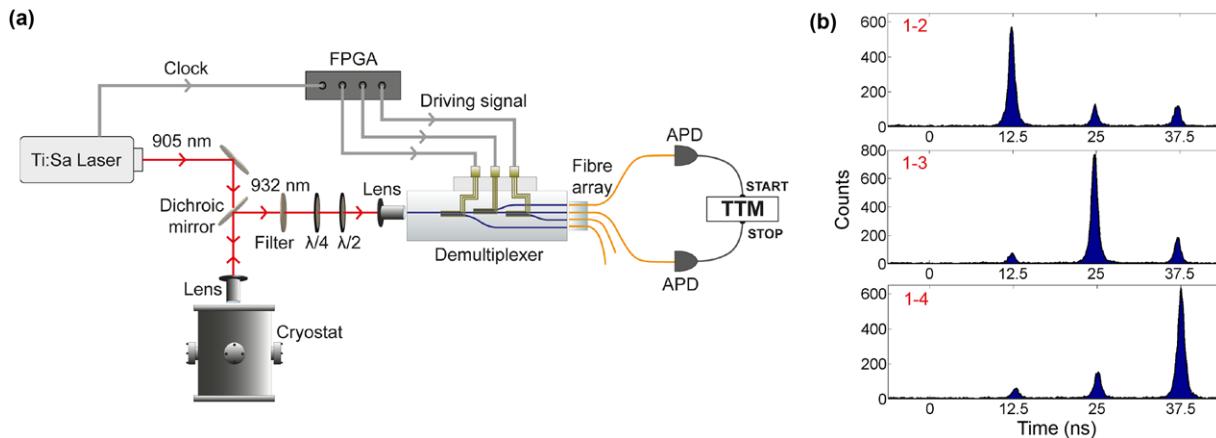
(a)

(b)

Figure 2 (a): Setup for the experimental implementation of the demultiplexing scheme (detailed description is given in the main text). (b): Time histograms for the two-photon coincidences between the first output and all other channels for a pump power $P = 660$ μW and a 2 minute acquisition time (waveguide numbering is from top to bottom).

Table 1 Splitting ratios of the directional couplers calculated from the data in Fig. 2b., with uncertainty from the fit confidence. Non-zero *off* values are caused by incorrect voltages from the pulse generator. Non-unity *on* values are caused by incorrect driving voltages and deviations from the desired coupling rate due to waveguide imperfections

switch	1	2	3
on	0.87 ± 0.06	0.94 ± 0.05	0.90 ± 0.06
off	0.06 ± 0.02	0.13 ± 0.03	0.13 ± 0.05

Figure 3 Comparison between the estimated photon rates at the output of the demultiplexer of an active ($\circ$) and probabilistic ($\square$) demultiplexing schemes for a state-of-the-art QD pumped under resonant excitation [8]. ($\diamond$) shows the rate of n heralded single photon sources with brightness of 0.75%. Inset shows the measured two-photon coincidence rates $c_p(2)$ as a function of the pump power P. Red line is the fit made with the saturation function given in the main text. Error bars are smaller than data points.

coincidence counts between the different channels. A non-zero switching voltage is necessary to compensate for fabrication imperfections.

To verify the correct operation of the switches, as well as their synchronization with the master laser, we first reconstruct the time histograms of two-photon coincidences counts between the first output of the demultiplexer and all other channels. The device is cyclically operated such that the first photon is sent to output one, the second to output two, and so on, and coincidences are measured between all four outputs simultaneously. Figure 2b shows the three time histograms (from a total of six pairwise combinations) of the coincidences measured by all four detectors. We observe enhanced peaks in coincidences at the corresponding delays of our demultiplexer, together with suppressed counts at different delays—showing the correct functioning of our device. The non-vanishing coincidence counts (smaller peaks) in the histograms arise from imperfect operation of the modulated couplers. From the data in Fig. 2b we calculated the splitting ratios of the three switches for both settings using a least-squares fitting procedure (see Table 1). The presence of non-zero *off* values and non-unity *on* values reveals the non-ideal operation of the device. The absence of counts at zero time delay (at the same level of accidental counts) is due to the low $g^2(0)$ value of the
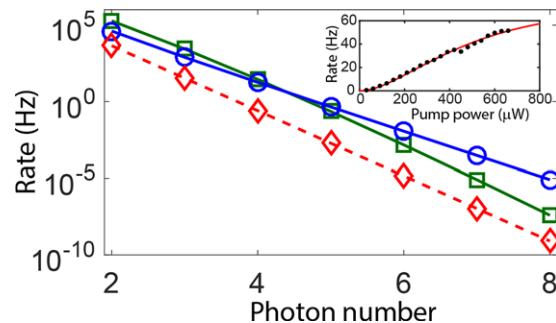
source, measured as $g^2(0) = 0.029 \pm 0.001$ at $P = 3P_0$ in [10].

The Inset of Fig. 3 shows the measured power-dependent rate of two-photon coincidences $c_{DM}(2)$ at outputs 1 and 2 of our demultiplexer. As expected for a QD pumped under quasi-resonant excitation it follows a saturation function $c_{DM}(2) = c_{max}(2)[1-\exp(-P/P_0)]^2$ quadratic in the P-dependence of the single-photon brightness. A fit to the data results in $c_{max}(2) = 70.9 \pm 3.0$ Hz, the maximum detected 2-photon rate, and $P_0 = 348 \pm 16$ μW the saturation power. We measured two-fold and three-fold photon coincidence rates of 65 ± 10 s^{-1} and 0.11 ± 0.02 s^{-1} at the output for a pump power $P = 660$ μW. The switching efficiency η_{DM} is finally estimated by fitting all ten combinations of two and three photon coincidence rates with Eq. 1, with $R = 80$ MHz, $\eta_{det} = 30\%$, and $\eta_{SD} = 0.76\%$ is calculated from the total

number of counts measured with the four detectors. We find an average switching efficiency $\eta_{DM} = 0.78 \pm 0.06$, in good agreement with the value $\eta_{DM} = 0.80 \pm 0.09$ predicted from the measured splitting ratios.

Four-fold coincidences were predicted to be 0.18 ± 0.06 mHz due to the low value of T in the current system, producing insufficient statistics in the acquisition time of 87 min. Dark counts of our detectors were ~ 300 Hz per detector, giving no significant contribution to coincidence mesurements.

To investigate the potential of our technology for the realisation of a multi-photon source with larger numbers we calculate the expected photon rates at the output of the demultiplexer for a state-of-the-art QD with 15% polarised brightness pumped under resonant-excitation [8]. The total transmission of our demultiplexer is tested by coupling the waveguide with a gaussian mode from an single-mode optical fibre and is found to be $T = 30\%$. This value is compatible with an overlap with the waveguide mode $\simeq 85\%$, as measured from mode imaging at the output of the waveguide, 14% Fresnel losses at the input and output facet and propagation losses $\simeq 0.65$ dB/cm and is the same value measured from a straight waveguide fabricated on the same chip, meaning that the couplers and electrodes did not introduce extra losses. In Fig. 3 we report the expected photon rates for increasing photon numbers calculated for a pump rate $R = 80$ MHz, $\eta_{DM} = 78\%$, and a transmission $T = 0.3/(0.86 \times 0.86)$ corrected for Fresnel losses, that can be eliminated with an anti-reflection coating at the input and output facets. The QD brightness is corrected by an additional loss factor 65% that takes into account the coupling efficiency of the QD emission mode to a single-mode fibre [10]. The proposed system with these parameters is expected to outperform a probabilistic demultiplexing scheme—made of a network of passive beam splitters with zero propagation losses– for a number of photons $n > 4$ and would enable a 6-photon rate $\simeq 0.01$ Hz, which is three orders of magnitude larger than what could be obtained with six heralded SPDC sources with equivalent quality and brightness of 0.075 [8] (see Fig. 3). The same calculation for a resonantly-excited QD with 14% brightness measured at the ouptut of a single-mode fibre [9], would enable, instead, a 6-photon rate $\simeq 0.1$ Hz. This technology offers great potential for further improvement, in particular by the use of the Reverse Proton exchange technique [12] for an improved coupling with optical fibres and reduced surface-scattering losses we estimate that we can achieve insertion losses lower than 3 dB. Furthermore the switching efficiency of the couplers can be increased with an optimized driving voltage and waveguide fabrication process. Such upgrades will enable the scaling of this platform to a larger number of photons.

In conclusion, we have proposed and experimentally implemented an example of active demultiplexing with a single integrated device of single-photons from a solid-state source. The performance of the demultiplexer has been analysed in conjunction with a QD pumped under quasi-resonant excitation and we have discussed the potential of our technology for state-of-the-art quantum dots. The proposed demultiplexing device is of general interest for any bright temporally distributed single-photon source and provides a scalable approach for the realisation of multi-photon sources of larger photon numbers. Our platform thus constitutes a very promising approach for scalable quantum photonics, in particular for protocols of intermediate—i.e., non universal—quantum computation, such as Boson Sampling [17–19], where, arguably, as few as seven photons from an actively demultiplexed quantum dot-based source could finally demonstrate the quantum advantage over classical systems [20].

References

[1] M. Barbieri, T. Weinhold, B. Lanyon, A. Gilchrist, K. Resch, M. Almeida, and A. White, Journal of Modern Optics **56**(2-3), 209–214 (2009).

[2] X. s. Ma, S. Zotter, J. Kofler, T. Jennewein, and A. Zeilinger, Phys. Rev. A **83**, 043814 (2011).

[3] M. Collins, C. Xiong, I. Rey, T. Vo, J. He, S. Shahnia, C. Reardon, T. Krauss, M. Steel, A. Clark, and B. Eggleton, Nat. Comms. **4**(2582), (2013).

[4] F. Kaneda, B. G. Christensen, J. J. Wong, H. S. Park, K. T. McCusker, and P. G. Kwiat, Optica **2**(12), 1010–1013 (2015).

[5] C. Xiong, X. Zhang, Z. Liu, M. J. Collins, A. Mahendra, L. G. Helt, M. J. Steel, D. Y. Choi, C. J. Chae, P. H. W. Leong, and B. J. Eggleton, Nat. Comms. **7**(10853), (2016).

[6] T. Meany, L. A. Ngah, M. J. Collins, A. S. Clark, R. J. Williams, B. J. Eggleton, M. J. Steel, M. J. Withford, O. Alibart, and S. Tanzilli, Laser Photon. Rev. **8**(3), L42–L46 (2014).

[7] G. J. Mendoza, R. Santagati, J. Munns, E. Hemsley, M. Piekarek, E. Martín-López, G. D. Marshall, D. Bonneau, M. G. Thompson, and J. L. O'Brien, Optica **3**(2), 127–132 (2016).

[8] N. Somaschi, V. Giesz, L. D. Santis, J. C. Loredo, M. P. Almeida, G. Hornecker, S. L. Portalupi, T. Grange, C. Antón, J. Demory, C. Gómez, I. Sagnes, N. D. Lanzillotti-Kimura, A. Lemaítre, A. Auffeves, A. G. White, L. Lanco, and P. Senellart, Nat. Photon. **10**, 340–345 (2016).

[9] X. Ding, Y. He, Z. C. Duan, N. Gregersen, M. C. Chen, S. Unsleber, S. Maier, C. Schneider, M. Kamp, S. Höfling, C. Y. Lu, and J. W. Pan, Phys. Rev. Lett. **116**, 020401 (2016).

[10] J. C. Loredo, N. A. Zakaria, N. Somaschi, C. Anton, L. de Santis, V. Giesz, T. Grange, M. A. Broome, O. Gazzano, G. Coppola, I. Sagnes, A. Lemaitre, A. Auffeves, P. Senellart, M. P. Almeida, and A. G. White, Optica **3**(4), 433–440 (2016).

[11] H. Wang, Z. C. Duan, Y. H. Li, S. Chen, J. P. Li, Y. M. He, M. C. Chen, Y. He, X. Ding, C. Z. Peng, C. Schneider, M. Kamp, S. Höfling, C. Y. Lu, and J. W. Pan, Phys. Rev. Lett. **116**, 213601 (2016).

[12] F. Lenzini, S. Kasture, B. Haylock, and M. Lobino, Opt. Express **23**, 1748–1756 (2015).

[13] H. F. Taylor, J. Appl. Phys. **44**, 3257 (1973).

[14] J. C. Loredo, M. A. Broome, P. Hilaire, O. Gazzano, I. Sagnes, A. Lemaitre, M. P. Almeida, P. Senellart, and A. G. White, arXiV:1603.00054 (2016).

[15] O. Gazzano, S. M. de Vasconcellos, C. Arnold, A. Nowak, E. Galopin, I. Sagnes, L. Lanco, A. Lemaître, and P. Senellart, Nature Communications **4**, 1425 (2013).

[16] B. Haylock, F. Lenzini, S. Kasture, P. Fisher, E. W. Streed, and M. Lobino, Rev. Sci. Instrum. **87**, 054709 (2016).

[17] S. Aaronson and A. Arkhipov, Proc. ACM Symposium on Theory of Computing, San Jose, CA p. 333 (2011).

[18] S. Aaronson, Proceedings of the Royal Society A: Mathematical, Physical and Engineering Science **467**, 3393 (2011).

[19] J. Huh, G. G. Guerreschi, B. Peropadre, J. R. McClean, and A. Aspuru-Guzik, Nat. Photon **9**, 615 (2015).

[20] L. Latmiral, N. Spagnolo, and F. Sciarrino, New J. Phys. **18**(11), 113008 (2016).